ORIGINAL PAPER

One-pot synthesis of various Ag–Au bimetallic nanoparticles with tunable absorption properties at room temperature

Brett W. Boote · Hongsik Byun · Jun-Hyun Kim

Abstract This report describes the formation of gold-coated silver bimetallic nanoparticles prepared by the one-pot synthetic approach which involves the subsequent reduction of silver and gold ions at ambient conditions. The reduction of silver ions by excess L-ascorbic acid initially led to the formation of silver cores. This step was followed by the addition of gold ions into the preformed cores, resulting in the formation of silver-core gold-shell type bimetallic nanoparticles at room temperature. This process systematically allowed for the formation of various bimetallic nanoparticles which exhibited tunable absorption properties corresponding to the visible and near-IR regions. The thickness of the gold shells and the diameter of the silver-core nanoparticles were readily controlled; the morphological and structural properties of the resulting bimetallic nanoparticles were thoroughly analyzed by SEM/TEM, DLS, and UV–Vis spectrophotometry. The overall results demonstrated not only that these gold-coated silver nanoparticles were reliably prepared by our one-pot synthetic approach, but also that their optical properties were tunable in the visible and near-IR areas as a function of the core size and shell thickness.

Keywords Bimetallic nanoparticles · Gold · Silver · Near infrared · Core–shell

B. W. Boote · J.-H. Kim (✉)
Department of Chemistry, Illinois State University, Normal,
IL 61790-4160, USA
e-mail: jkim5@ilstu.edu

H. Byun
Department of Chemical System Engineering, Keimyung
University, Daegu 704-701, South Korea
e-mail: hsbyun@kmu.ac.kr

Introduction

The preparation of metal nanoparticles in small sizes that absorb in the visible and near-IR spectral regions remains an ongoing challenge to colloidal science [1, 2]. Access to these broad absorption areas is especially important for solar energy based and/or biological applications because optically driven solar cells and therapies represent some of the most promising advances in the emerging field of renewable energy systems and nanomedicine [3, 4]. These developing nanotechnologies take advantage of the fact that there are not many chromophores in biological tissue that broadly absorb in the visible and near-IR regions [5, 6]. As such, metal nanoparticles are often preferred over organic-based systems because of the tunable and strong absorption bands from the visible to near-IR areas, as well as their extended stability in solutions and/or solid states [7–9].

Numerous studies have proposed strategies to construct or transform metal nanoparticles into diverse nanostructures (including prisms, disks, rods, and core–shells) that can tune the absorption properties [10–14]. In particular, the preparation of metal–metal core–shell nanoparticles possessing desired optical and electrical properties with a biocompatible nature have been extensively studied by the subsequent chemical reduction method using two or more metal ions [9, 13, 15–20]. Moreover, controlling the absorption properties of these nanoparticles on a sub-100-nm scale may bring additional advantages for practical use in biotechnology and photoinduced reactions due to their high surface-to-volume ratio. Unfortunately, most preparation methods for such nanoparticles often require high-reaction temperatures, multiple steps, and/or the proper use of unique stabilizing agents [21–26]. Here, we demonstrate a simple one-pot synthetic method that allows for the reliable preparation of stable core–shell type bimetallic nanoparticles with strong and tunable optical properties at ambient conditions. Specifically, two different sizes

of Ag core nanoparticles (~15 and ~40 nm in diameter) were prepared at room temperature and used as cores for Au shells. Varying thicknesses of Au shells were grown on the Ag cores simply by adding selected amounts of $HAuCl_4$ in a potassium carbonate (K_2CO_3) solution to an aqueous solution of the preformed Ag cores in situ. The absorption wavelengths of these "core–shell type bimetallic nanoparticles" can be systematically tuned from the visible to the near-IR region by adjusting the molar ratio of the initial reagents. Importantly, these bimetallic nanoparticles are reliably prepared and can be modified further with substantially greater ease and more anisotropic shapes than the related gold-coated dielectric or metallic nanoshells/nanocubes [11, 13, 14, 20, 27–29]. Upon the formation of various bimetallic nanoparticles possessing a strong and broad absorption band, these nanoparticles may serve as interesting materials in the area of optically tunable devices, SERS enhancers, and biomedical applications [15, 30–34].

Experimental section

Materials Nitric acid, hydrochloric acid, potassium hydroxide, isopropyl alcohol, methanol, ethanol, hexadecyltrimethylammonium bromide (CTAB, ≥99.0 %) (all from Fisher Scientific), potassium carbonate (≥99.0 %), sodium borohydride (~98 %), hydrogen tetrachloroaurate(III) hydrate (99.999 % trace metals basis), L-ascorbic acid (AsA, ≥99.0 %) (all from Aldrich), and silver nitrate (from Mallinckrodt) were used without purification from the indicated commercial suppliers. Deionized water was purified to a resistance of 18 MΩ (Nanopure Water System; Barnstead/Thermolyne) and filtered through a 0.2 μm membrane to remove impurities. All glassware was cleaned with an aqua regia solution, followed by treatment in a base bath, and then rinsed with pure water prior to use.

Characterization methods All nanoparticles were characterized by ultraviolet–visible (UV–Vis) spectroscopy for the absorption properties, by environmental scanning electron microscopy (SEM) and transmission electron microscopy (TEM) for the morphology and structure, and by dynamic light scattering (DLS) for the size distribution.

An FEI Quanta 450 instrument operating at 20 kV and Zeiss 10 TEM operating at an accelerating voltage of 80 kV were used to evaluate the general size distribution and the overall structure of the nanoparticles, respectively. All samples were deposited from solution onto silicon wafers (for SEM) and 300 mesh carbon-coated copper grids (for TEM) and then completely dried at room temperature overnight.

DLS on a ZetaPALS equipped with a particle analyzer (Brookhaven Instruments Corp., Holtsville, New York) with a 35 mW solid-state laser (90 and 15° angular measurements) was employed to examine the hydrodynamic diameter and

polydispersity of the nanoparticles as well as zeta potentials. The diameters were collected at 20 °C from an average of five measurements over 100 s.

An Agilent 8453 UV–Vis spectrometer was used to characterize the absorption properties of the nanoparticles over the wavelength range of 200 to 1,100 nm. All samples were prepared in pure water and transferred to a quartz UV–Vis cell.

Preparation of $HAuCl_4$ and $AgNO_3$ stock solution All preparation methods involved the use of $HAuCl_4$ or $AgNO_3$ in a K_2CO_3 solution (the K–Au solution and K–Ag solution, respectively). Specifically, the preparation of the K–Au solution was as follows: 0.025 g of K_2CO_3 and 98 mL of water were added to a 150 mL Erlenmeyer flask. The solution was stirred for at least 15 min to completely dissolve the K_2CO_3, followed by the rapid addition of 2 mL of 1 wt.% $HAuCl_4$ H_2O solution. The color of the mixture changed from light yellow to colorless within 30 min. In the case of the K–Ag solution, 1 mL of 1 wt.% $AgNO_3$ was introduced to an aqueous 99 mL solution of K_2CO_3, which exhibited a color change from colorless to bright yellow in a few seconds. The final solutions were stored overnight in a refrigerator prior to use.

Preparation of large Ag core–Au shell nanoparticles Five milliliter of the prepared K–Ag solution was placed in a 20 mL glass vial containing a magnetic stirring bar. L-ascorbic acid (0.3 mL of 100 mM: 0.176 g/10 mL water) was quickly introduced to the yellow K–Ag solution, resulting in the formation of Ag nanoparticles with a greenish yellow color. Subsequently, varying amounts of K–Au solution were slowly (dropwise) or rapidly introduced into the mixture. The final solution was stirred for an additional 5 min and exhibited a reddish-yellow to brownish-blue color as a function of the concentration of the K–Au solution.

Preparation of small Ag core–Au shell nanoparticles Five milliliter of the prepared K–Ag solution (2.94 μmol) was placed in a 20 mL glass vial containing a magnetic stirring bar. $NaBH_4$ (0.02 mL of 3.2 mM: 1.2 mg/10 mL of water) was quickly added to the yellow K–Ag solution to form small Ag seed nanoparticles. Subsequently, L-ascorbic acid (0.3 mL of 100 mM) was added to the reaction mixture, resulting in the formation of small dark yellow Ag cores that were presumably prepared through the seed growth process. Varying amounts of the K–Au solution were then slowly (dropwise) introduced into the mixture. The final solution was stirred for an additional 5 min; it exhibited a reddish-yellow to brownish-blue color as a function of the concentration of the K–Au solution.

Transformation of the Ag–Au core–shells into large uniform or anisotropic structures under light irradiation Ten milliliter of preheated hexadecyltrimethylammonium bromide

solution (CTAB, 10 mM, 0.0364 g in 10 mL water, ≥35 °C) was placed in a 15 mL polystyrene centrifuge tube. Subsequently, $HAuCl_4$ (0.2 mL of 1 wt.% solution) was added, and the tube was swirled several times, resulting in a homogeneous orange color. L-ascorbic acid (0.6 mL of 100 mM) was quickly added to the orange solution, which led to a colorless solution. Finally, an aliquot of preformed 0.4 M ratio bimetallic core–shell nanoparticles (0.1–0.5 mL) was added to the colorless solution; the tube was capped loosely and then placed under fluorescent light irradiation (a 35 W desk lamp at a distance of 5 cm providing 100 mW/cm^2, as measured by a handheld optical power meter; Newport Corp.) for 30 min. The final solution was centrifuged at 3,000 rpm twice, and the precipitates were resuspended in 3 mL of pure water. The final colors of the solutions were brownish-red under reflection and deep blue under transmission.

Results and discussion

Various Ag–Au core–shell type bimetallic nanoparticles prepared by our developed one-pot synthetic approach largely cover from the visible to the near-IR range simply by adjusting the ratio of the initial silver and gold ions. The small Ag core nanoparticles ~15 nm diameter and large Ag core nanoparticles ~40 nm in diameter were prepared by the reduction of Ag ions (K–Ag) with the combination of $NaBH_4$ and AsA at ambient conditions. Subsequently, these core nanoparticles were coated with tunable Au layers through the introduction of varying amounts of the Au growth solution (K–Au) in the presence of a residual reducing agent (i.e., AsA). The systematic control of the diameters of these nanoparticles allowed for tunable absorption properties depending on the core size and the shell thickness. This entire process was systematically completed in situ one-pot at room temperature. Interestingly, the rate of adding the K–Au growth solution (slow vs. rapid) to the Ag seed nanoparticles slightly affected the reproducible formation, the surface morphology, and the absorption bands of the resulting nanoparticles. Based on previous studies, the reduction of Au ions in the presence of preformed Ag cores generally led to the formation of Ag-rich cores and Ag–Au alloy shells with compositions that were enriched in the gold component with the increasing Au mole fraction [18, 35, 36]. Although understanding the precise compositions of these bimetallic nanoparticles is important, the main goals of this research were to demonstrate a simple synthetic method for the preparation of various sub-100-nm bimetallic nanoparticles and the subsequent modification of these core–shells to possess tunable absorption properties. As such, these Ag core–Au shell type bimetallic nanoparticles were examined as a function of the Ag and Au molar ratio from 0.1 to 1.0 (K–Au/K–Ag). To the best of our knowledge, this is the first study to demonstrate the reliable formation of the Ag–Au core–shell nanoparticles in the absence of a surfactant at room temperature via a one-pot synthetic approach.

Figures 1 and 2 show the SEM and TEM images of the relatively large and rough Ag core nanoparticles and the core–shell nanoparticles of varying thicknesses that were prepared by the subsequent reduction of Ag and Au ions in the presence of an excess reducing agent. The irregular and polydisperse Ag cores ~40 nm in diameter (~0.30 PDI by DLS) were initially formed by the reduction of Ag ions at a high pH (pH ~10) with excess AsA. This result is similar to previous studies that demonstrated the formation of rough and partially aggregated nanoparticles upon the reduction of metal ions with excess AsA in the absence of a surfactant [37–40]. After a short period of time (≤5 min), the K–Au solution was subsequently introduced either slowly (i.e., dropwise) or rapidly to the solution containing these preformed Ag core nanoparticles. This process allowed for the gradual coating of gold layers around the Ag cores. We noted that the nanoparticles prepared by rapid addition exhibited slightly rougher, more irregular structures (as well as partial aggregation) than those formed through the slow addition of the solution. The thickness of the shell was estimated by comparing the total diameter of the nanoparticles before and after the shell growth. The nanoparticles prepared by both methods at or below room temperature generally showed rough and irregular shapes. These results were comparable to the previous nanocube system, in which the rougher Au coating was often accomplished on preformed Ag nanocubes at a low temperature (i.e., 20 °C) rather than a high temperature (i.e., 100 °C) [25]. In addition to the low temperature, it is also important to remember that such rough core–shell type nanoparticles could also be affected by the presence of excess AsA, which could cause the formation of rough and partially aggregated nanoparticles [37, 39, 41, 42]. As the amount of the K–Au solution increased, the size of the core–shell nanoparticles systematically increased, probably due to the thicker coating of the Au layer. When excess K–Au solution (over a 1:1 ratio of K–Au to Ag seed solution) was introduced into the preformed Ag seed solution, the Au shell layer was too thick to clearly visualize the core–shell structures, even with TEM analysis. The highly reproducible and consistent formation of the Ag core–Au shell particles was observed when the molar ratio between the K–Au growth solution and the Ag seed solution was higher than 0.4 for the rapid addition and 0.3 for the slow addition of the solution, respectively. While newly formed small Au nanoparticles and the increased aggregation of the nanoparticles were often observed under the rapid addition condition (zeta potentials of the nanoparticles, from −25 to −35 mV, implied stable colloids in solution, but partially aggregated nanoparticles were often observed), the slow addition process generally allowed for the more reliable and gradual coating of Au layers around the preformed Ag core nanoparticles.

A UV–Vis spectrophotometer was employed to monitor the absorption patterns of the core–shell nanoparticles prepared by subsequent rapid or dropwise addition of varying amounts of the K–Au growth solution to the preformed Ag nanoparticles (Fig. 3a, b). The K–Ag solution initially showed a very weak absorption peak at ~400 nm (data not shown). Upon the addition of excess AsA, an intense and broad absorption band appeared at ~410 nm, indicating the formation of rough and polydisperse Ag nanoparticles. At a ratio of 0.1 of the K–Au growth solution to Ag cores, a notably decreased absorption intensity of the Ag cores occurred at ~410 nm and a new peak forms at ~500 nm under both conditions, which were presumably caused by the formation of Ag–Au alloy shells on Ag core nanoparticles. As the ratio of the K-Au solution to Ag seed solution increased, the gradual decrease of the strong Ag core peak at ~410 nm and new absorption bands at longer wavelengths between typical pure gold and silver nanoparticles with a shoulder peak clearly suggested the formation of Au–Ag alloy shells on Ag cores. It has been reported that a certain degree of alloying occurs during the reduction of Au ions in the presence of Ag seeds [13, 36]. At the ratio of 0.3, a peak centered at ~654 nm with a broad shoulder peak below

~500 nm still pointed to a Ag core on a Au–Ag alloy shell. When the ratio reached 0.5, the longest absorption band centered at ~700 nm without a notable shoulder peak below ~500 nm was observed, probably for the Ag-rich core and Au-rich shell nanoparticles. The absorption peaks were then slightly blue-shifted as the ratios of the K–Au solution to Ag core solution increased above a molar ratio of 0.5. A further increase of the ratio over 1.0 resulting in the slight red-shift of the absorption band again suggested the increase in the nanoparticle diameters [43, 44], which was consistent with the SEM images and DLS size measurements. Unlike the rapid addition method, slightly narrower absorption bands of the core–shell nanoparticles prepared by the slow addition process might suggest a smoother (less rough) surface of the Au layers on the Ag cores with fewer partial aggregations.

Interestingly, the absorption bands of the nanoparticles prepared by the slow addition remained similar, but the adsorption bands of the nanoparticles prepared by the rapid addition were gradually blue-shifted (shift of λ_{max}, 5–10 nm) and became narrow upon aging at room temperature for over 2 days. This observation might be explained by the possible surface restructuring process of the nanoparticles [39, 40].

Fig. 1 SEM/TEM images of **a** K–Ag cores and Ag–Au core-shells with **b** 0.3, **c** 0.5, and **d** 1.0 Au/Ag molar ratios (slow addition)
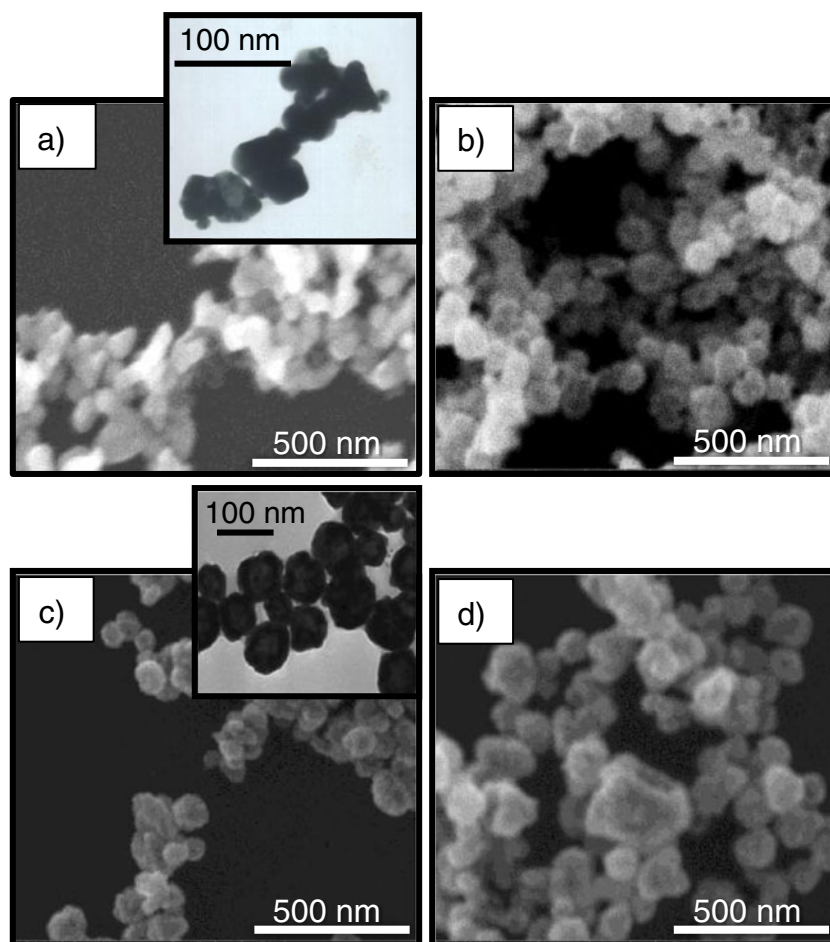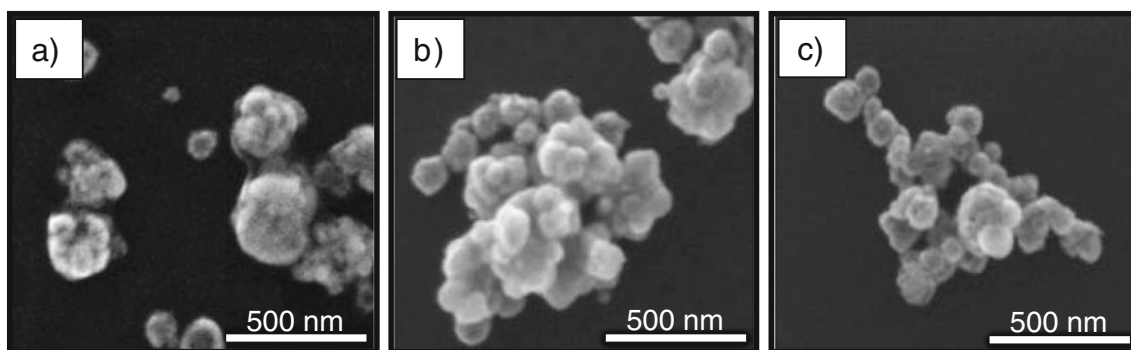
Fig. 2 SEM images of Ag–Au core–shells with **a** 0.3, **b** 0.5, and **c** 1.0 Au/Ag molar ratios (rapid addition)

Based on our previous studies, partially aggregated gold nanoparticles with a rough surface prepared by excess AsA underwent a notable reshaping process upon aging at room temperature to form polydisperse gold nanoparticles with a smooth surface. This morphological evolution of the gold nanoparticles was able to be thoroughly examined by the significantly blue-shifted absorption maxima and overall absorption patterns [37, 39, 40]. Although we did not microscopically observe the differences in the surface roughness, the slight shift in the absorption bands for our core-shell nanoparticles as a function of time could explain our speculation for the change in the surface structures. In a separate study done by Moskovits and his group, the blue-shift of the absorption bands and less roughness of the nanoparticles might be affected by the slow reduction of the adsorbed Au ions on the surface of the nanoparticles as well [45]. As such, it was clear that the addition rate of the Au growth solution to the preformed Ag cores played an important role in the reproducible formation, the surface morphology, and the absorption property of the resulting core–shell type bimetallic nanoparticles. We are still investigating the main cause of

the slight shift of the absorption bands of the nanoparticles prepared by the rapid addition process.

An additional feature of our core–shell type bimetallic nanoparticles was that the nanoparticles did not exhibit severe pinholes or hollow interiors as well as any destruction (i.e., the Ag atoms were dissolved by $HAuCl_4$) regardless of the addition rate of the Au growth solution. The formation of Ag–Au core–shell nanoparticles is often accomplished via the galvanic replacement reaction when an Au growth solution is introduced to citrate-stabilized Ag core nanoparticles in the absence of reducing agents [13, 25]. The final core–shell nanoparticles readily possess pinhole/hollow structures due to the galvanic reaction of the Ag core nanoparticles by $AuCl_4^-$ ions. A similar reaction process was also observed by the Xia group during the formation of hollow Au nanocages on Ag core nanoparticles via the polyol method at high temperatures. As the amount of the Au growth solution increased, a dealloying process typically took place in the absence of reducing agents [25]. Upon this dealloying process, the broad absorption band of the nanoparticles flattened/disappeared due to the destruction of the core–shell
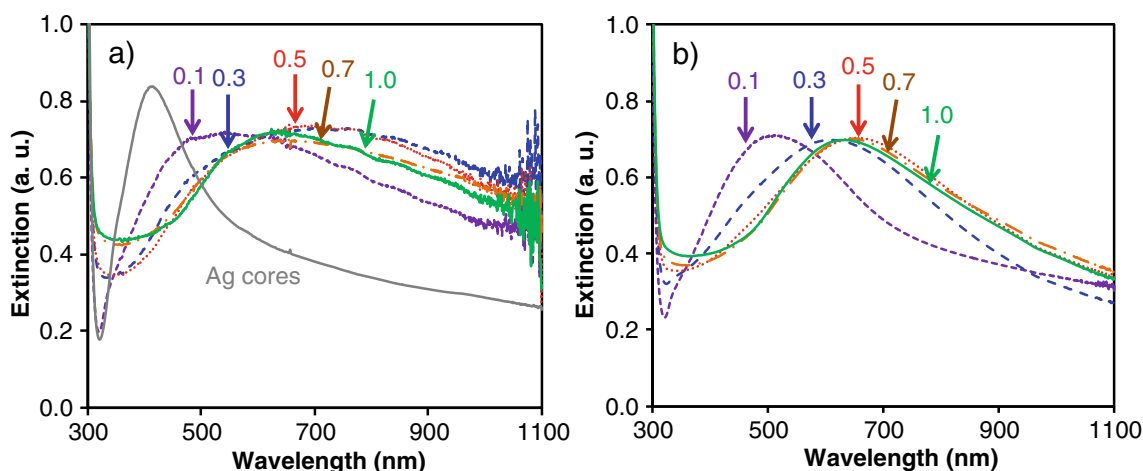

Fig. 3 UV–Vis spectra of various Ag–Au core–shells noted by initial Au/Ag molar ratio using the **a** rapid addition of K–Au and **b** slow addition of K–Au

structures. However, since our core–shell nanoparticles were prepared in the presence of a high concentration of residual AsA, the reduction of Au ions on the preformed Ag core nanoparticles by AsA was speculated to be preferred over the galvanic reaction process because our core–shell nanoparticles were less likely to exhibit pin holes or hollow structures. Additionally, the formation of a thicker gold coating was easily achieved rather than the rapid dealloying of the nanoparticles with an increase of the K–Au solution. The maintenance of strong and broad absorption peaks even after the addition of excess K–Au solution (i.e., a two times greater concentration) strongly supported the preservation of the Ag–core and Au-rich shell type structures under our reaction conditions. In a separate study, Liz-Marzan and his group also proposed the favorable reduction of Au ions on preformed Ag seeds in the presence of AsA as a reducing agent [18, 46].

The slow (dropwise) addition of the K–Au solution onto Ag core nanoparticles yielded the reliable formation of a slightly smooth surface and less aggregation of the bimetallic nanoparticles. The small Ag seed nanoparticles (~2–3 nm in diameter) were initially formed by the reduction of Ag ions with a strong reducing agent (NaBH$_4$); this led to a bright yellow color. This was followed by the subsequent addition of excess AsA, resulting in the formation of polydisperse Ag nanoparticles ~15 nm in diameter (~0.35 PDI by DLS) at room temperature via the seed growth process. A selected amount of the K–Au solution was then slowly introduced to

these preformed Ag nanoparticles to prepare various Au shells on small Ag cores. Figure 4 shows the SEM and TEM images of the small Ag core nanoparticles and Ag–Au core–shell nanoparticles with varying shell thicknesses. While bare Ag core nanoparticles initially exhibited slightly irregular shapes with partial aggregation, the core-shell bimetallic nanoparticles showed the systematic increase in the diameters of the nanoparticles, suggesting the successful growth of Au shells. The TEM image (Fig. 4b) again clearly shows two different contrasts throughout the nanoparticles coming from the phase boundary between the Au shell and Ag core. The apparent core–shell contrast consisting of darker outer shells and the lighter inner cores originated from the gold and silver elements because gold scatters more electrons than silver [47]. Such a contrast in the Ag–Au core–shell structures has also been observed in other studies as well [35, 47, 48], which were consistent with our results and confirmed the successful growth of Au layers on small Ag core nanoparticles with increased surface-to-volume ratios.

The absorption spectra of the small core–shell nanoparticles were collected before and after the growth of various thicknesses of the Au shells (Fig. 5). The introduction of an aliquot of NaBH$_4$ initially led to the formation of small Ag seeds possessing a very weak absorption peak at 390 nm; the subsequent addition of excess AsA resulted in the further reduction of residual Ag ions to complete the growth of Ag nanoparticles possessing an intense absorption band at 400 nm with a broad

Fig. 4 SEM/TEM images of **a** 15 nm Ag cores and small Ag–Au core–shell particles with **b** 0.3, **c** 0.5, **d** 1.0 Au/Ag molar ratios
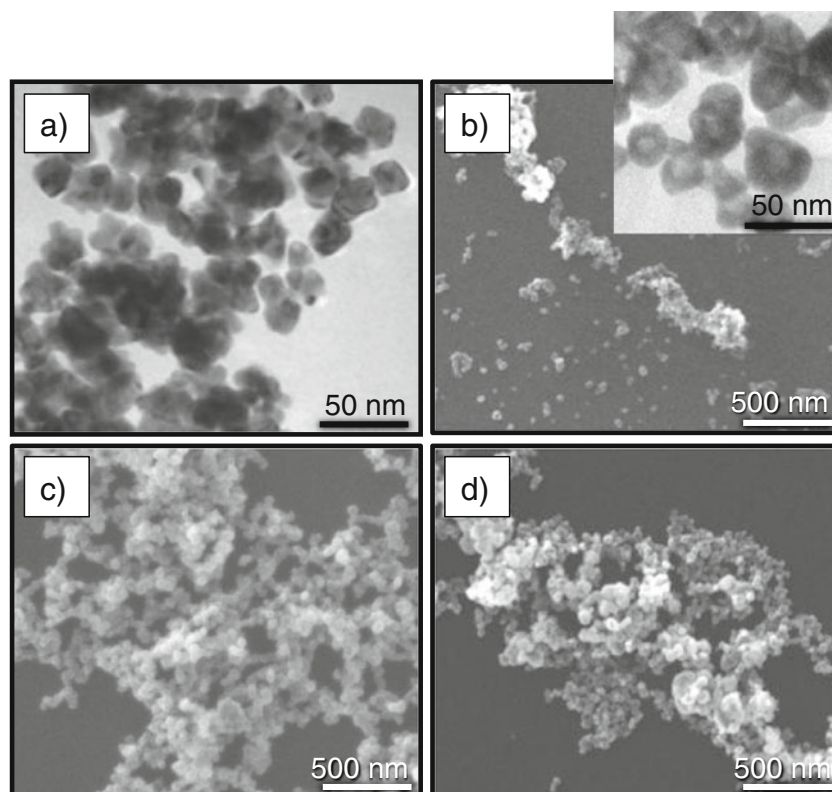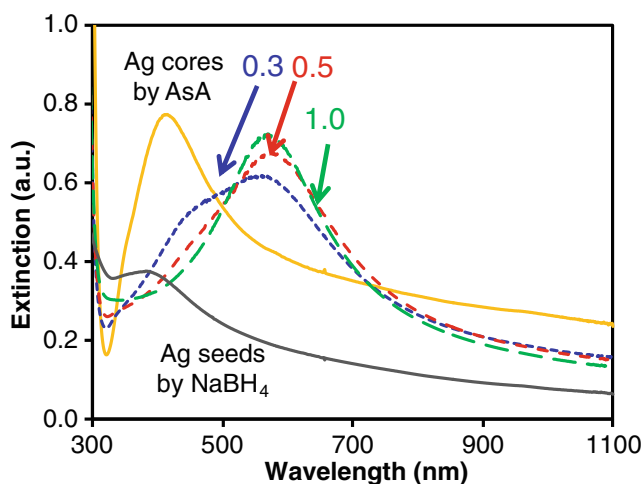
Fig. 5 UV–Vis spectra of small Ag cores and various core–shells prepared by different Au/Ag molar ratios

shoulder peak in the visible range. This broad absorption pattern of the resulting nanoparticles suggested the formation of rough polydisperse nanoparticles, which was consistent with the microscopic images. Upon the slow addition of the K–Au solution to these preformed Ag nanoparticles, the gradual decrease of the Ag core peak at 400 nm and the appearance of new peaks at over 550 nm indicated the formation of Ag–Au alloy type core–shell nanoparticles. As a small shoulder peak below 500 nm appeared as a result of the use of a 0.5 M ratio of K–Au to K–Ag, the small Ag cores required slightly more of the K–Au solution to form a Au-rich shell. The maximum absorption bands of the core–shell nanoparticles prepared by greater than 0.5 M ratios were placed in the visible (550–600 nm) range regardless of the shell thickness due to the relatively small size of the cores [45, 49], which is comparable to the
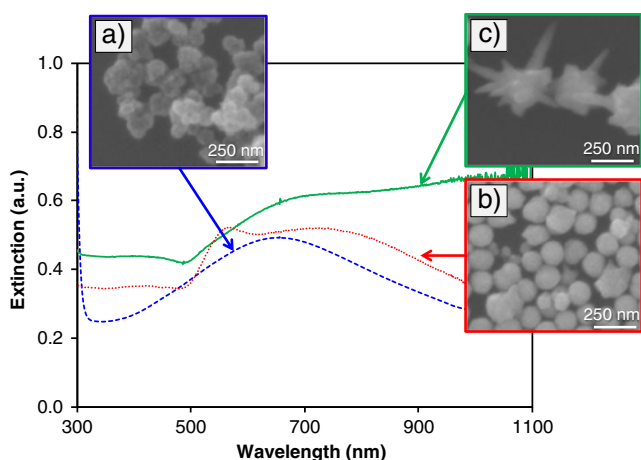

Fig. 6 UV–Vis spectra and corresponding SEM images of the transformation of 0.4 M ratio core–shells into large uniform or anisotropic structures. Note that the final structures of the particles vary based on the core–shell concentration

previous studies done by the Henglein (~8 nm core) [23] and Srnova-Sloufova (~9 nm core) [35] groups. The Liz-Marzan group prepared multiple core–shell structures using 17 nm core nanoparticles [18], and these nanoparticles also possessed limited absorption bands in the visible areas. However, our nanoparticles possessing highly increased surface-to-volume ratios exhibited slightly broader absorption bands (400–700 nm) than those of the precedent core–shell nanoparticles (400–600 nm), perhaps due to the roughness of the shells and their high polydispersity.

In addition, the resulting nanoparticles were found to be stable in the absence of any surfactants that provided great potential for easy modifications and/or applications. As a proof-of-concept example, the pre-synthesized large core–shell particles were transformed into either large uniform or anisotropic structures to completely cover broad absorption bands across the visible and near-IR areas. This modification process was simply accomplished by the addition of an aliquot of the core–shell particles (1 and 5 % seed particles to growth solution) into a fixed growth solution containing HAuCl$_4$, AsA, and a surfactant (CTAB), then exposed to visible light irradiation for 30 min. Figure 6 shows the SEM images of the initial core–shell particles and the transformed large uniform and anisotropic nanoparticles. Interestingly, the structures of the final nanoparticles were highly affected by the initial ratios of the core–shell nanoparticles to the growth solution. While symmetric growth was favored with the use of a high concentration of the core–shell nanoparticles, anisotropic growth was observed with a low concentration of the nanoparticles. The large uniform nanoparticles (~200 nm in diameter) exhibited two distinctive peaks at 560 nm for multipole resonance and at 760 nm for the dipole plasmon band, these peaks were consistent with those of large bare gold nanoparticle systems [50]. The highly anisotropic nanoparticles have shown a much broader absorption band across visible to near-IR range that is comparable to the previous work as well [51]. More thorough study is underway to elicit the concentration-related structural information.

Conclusions

The Ag–Au core–shell type bimetallic nanoparticles with varying sizes were reliably prepared by a very simple one-pot synthetic approach at ambient conditions. The thorough characterization of these nanoparticles by UV–Vis spectroscopy, SEM, DLS, and TEM collectively supported the reliable formation of various Ag–Au core–shells with tunable optical properties. Furthermore, the easy transformation of these nanoparticles into either large uniform or anisotropic structures under light irradiation can allow for their potential applications requiring strong optical properties in the visible and/or near-IR regions of the spectrum.

References

1. Daniel M-C, Astruc D (2004) Gold nanoparticles: assembly, supramolecular chemistry, quantum-size-related properties, and applications toward biology, catalysis, and nanotechnology. Chem Rev 104:293–346

2. El-Sayed MA (2004) Small is different: shape-, size-, and composition-dependent properties of some colloidal semiconductor nanocrystals. Acc Chem Res 37:326–333

3. Gobin AM, O'Neal DP, Watkins DM, Halas NJ, Drezek RA, West JL (2005) Near infrared laser-tissue welding using nanoshells as an exogenous absorber. Las Surg Med 37:123–129

4. Loo C, Lowery A, Halas N, West J, Drezek R (2005) Immunotargeted nanoshells for integrated cancer imaging and therapy. Nano Lett 5:709–711

5. Nie SR, Emroy SR (1997) Probing single molecules and single nanoparticles by surface-enhanced Raman scattering. Science 275:1102–1106

6. O'Neal DP, Hirsch LR, Halas NJ, Payne JD, West JL (2004) Photothermal tumor ablation in mice using near infrared-absorbing nanoparticles. Cancer Lett 109:171–176

7. Busbee BD, Obare SO, Murphy CJ (2003) An improved synthesis of high aspect ratio gold nanorods. Adv Mater 15:414–416

8. Wu H-Y, Huang W-L, Huang MH (2007) Direct high-yield synthesis of high aspect ratio gold nanorods. Crystal Growth & Design 7:831–835

9. Chaudhuri GR, Paria S (2012) Core/shell nanoparticles: classes, properties, synthesis mechanisms, characterization, and applications. Chem Rev 112:2373–2433

10. Averitt RD, Westcott SL, Halas NJ (1999) Linear optical properties of gold nanoshells. J Opt Soc Am B 16:1824–1832

11. Devi P, Badllescu S, Packlrlsamy M, Jeevanandam P (2010) Synthesis of gold-poly (dimethylsiloxane) nanocomposite through a polymer-mediated silver/gold galvanic replacement reaction. Gold Bull 43:307–315

12. Kim J-H, Bryan WW, Lee TR (2008) Preparation, characterization, and optical properties of gold, silver, and gold–silver alloy nanoshells having silica cores. Langmuir 24:11147–11152

13. Sun Y, Wiley B, Li Z-Y, Xia Y (2004) Synthesis and optical properties of nanorattles and multiple-walled nanoshells/nanotubes made of metal alloys. J Am Chem Soc 126:9399–9406

14. Wang W, Pang Y, Yan J, Wang G, Suo H, Zhao C, Xing S (2012) Facile synthesis of hollow urchin-like gold nanoparticles and their catalytic activity. Gold Bull 45:91–98

15. Liu X, Knauer M, Ivleva NP, Niessner R, Haisch C (2010) Synthesis of core–shell surface-enhanced Raman tags for bioimaging. Anal Chem 82:441–446

16. Mott D, Lee J, Thuy NTB, Aoki Y, Singh P, Maenosono S (2011) A study on the plasmonic properties of silver core gold shell nanoparticles: optical assessment of the particle structure. Japanese J App Phys 50:p065004–p065011

17. Pande S, Ghosh SK, Praharaj S, Panigrahi S, Basu S, Jana S, Pal A, Tsukuda T, Pal T (2007) Synthesis of normal and inverted gold–silver core–shell architectures in B-cyclodextrin and their applications in SERS. J Phys Chem C 111:10806–10813

18. Rodriguez-Gonzalez B, Burrows A, Watanabe M, Kielyb CJ, Liz-Marzan LM (2005) Multishell bimetallic AuAg nanoparticles: synthesis, structure, and optical properties. J Mater Chem 15:1775–1759

19. Vongsavat V, Vittur BM, Bryan WW, Kim J-H, Lee TR (2011) Ultrasmall hollow gold–silver nanoshells with extinctions strongly red-shifted to the near-infrared. ACS Appl Mater Interfaces 3:3616–3624

20. Xu W, Niu J, Shang H, Shen H, Ma L, Li LS (2013) Facile synthesis of AgAu alloy and core/shell nanocrystals by using Ag nanocrystals as seeds. Gold Bull 46:19–23

21. Anandan S, Grieser F, Ashokkumar M (2008) Sonochemical synthesis of Au–Ag core–shell bimetallic nanoparticles. J Phys Chem C 112:15102–15105

22. Chen Y-H, Nickel U (1993) Superadditive catalysis of homogeneous redox reactions with mixed silver–gold colloids. J Chem Soc Faraday Trans 89:2479–2485

23. Mulvaney P, Giersig M, Henglein A (1993) Electrochemistry of multilayer colloids: preparation and absorption spectrum of gold-coated silver particles. J Phys Chem 97:7061–7064

24. Radziuk D, Shchukin D, Mohwald H (2008) Sonochemical design of engineered gold–silver nanoparticles. J Phys Chem C 112:2462–2468

25. Sun Y, Xia Y (2004) Mechanistic study on the replacement reaction between silver nanostructures and chloroauric acid in aqueous medium. J Am Chem Soc 126:3892–3901

26. Treguer M, de Cointet C, Remita H, Khatouri J, Mostafavi M, Amblard J, Belloni J (1998) Dose rate effects on radiolytic synthesis of gold–silver bimetallic clusters in solution. J Phys Chem B 102:4310–4321

27. Brongersma ML (2003) Nanoshells: gifts in a gold wrapper. Nature Materials 2:296–297

28. Oldenburg SJ, Jackson JB, Westcott SL, Halas NJ (1999) Infrared extinction properties of gold nanoshells. Appl Phys Lett 75:2897–2899

29. Salgueirino-Maceira V, Caruso F, Liz-Marzan LM (2003) Coated colloids with tailored optical properties. J Phys Chem B 107:10990–10994

30. Chen J, Wang D, Xi J, Au L, Siekkinen A, Warsen A, Li Z-Y, Zhang H, Xia Y, Li X (2007) Immuno gold nanocages with tailored optical properties for targeted photothermal destruction of cancer cells. Nano Lett 7:1318–1322

31. Cui Y, Ren B, Yao J-L, Gu R-A, Tian Z-Q (2006) Synthesis of Ag core-Au-shell bimetallic nanoparticles for immunoassay based on surface-enhanced Raman spectroscopy. J Phys Chem B 110:4002–4006

32. Pavan Kumar GV, Shruthi S, Vibha B, ARB A, Kundu TK, Narayana C (2007) Hot spots in Ag core-Au shell nanoparticles potent for surface-enhanced Raman scattering studies of biomolecules. J Phys Chem C 111:4388–4392

33. Prevo BG, Esakoff SA, Mikhailovsky A, Zasadzinski JA (2008) Scalable routes to gold nanoshells with tunable sizes and response to near-Infrared pulsed-laser irradiation. Small 4:1183–1195

34. Stern JM, Stanfield J, Kabbani W, Hsieh J-T, Cadeddu JA (2008) Selective prostate cancer thermal ablation with laser activated gold nanoshells. J Urology 179:748–753

35. Srnova-Sloufova I, Lednicky F, Gemperle A, Gemperlova J (2000) Core–shell (Ag)Au bimetallic nanoparticles: analysis of transmission electron microscopy images. Langmuir 25:9928–9935

36. Srnova-Sloufova I, Vlckova B, Bastl Z, Hasslett TL (2004) Bimetallic (Ag)Au nanoparticles prepared by the seed growth method: two-dimensional assembling, characterization by energy dispersive X-ray analysis, X-ray photoelectron spectroscopy, and surface enhanced Raman spectroscopy, and proposed mechanism of growth. Langmuir 20:3407–3415

37. Kim J-H, Lavin BW (2011) Preparation of gold nanoparticle aggregates and their photothermal heating property. J Nanosci Nanotechnol 11:45–52

38. Kim J-H, Lavin BW, Boote BW, Pham JA (2012) Photothermally enhanced catalytic activity of partially aggregated gold nanoparticles. J Nanopart Res 14:p995–p1004

39. Kuo C-H, Huang MH (2005) Synthesis of branched gold nanoparticles by a seeding growth approach. Langmuir 21:2012–2016

40. Wu H-Y, Liu M, Huang MH (2006) Direct synthesis of branched gold nanocrystals and their transformation into spherical nanoparticles. J Phys Chem B 110:19291–19294

41. Andreescu D, Sau TK, Goia DV (2006) Stabilizer-free nanosized gold sols. J Colloid Interface Sci 298:742–751

42. Goia DV, Matijevic E (1998) Preparation of monodispersed metal particles. New J Chem 22:1203–1215

43. Haiss W, Thanh NT, Jenny Aveyard J, Fernig DG (2007) Determination of size and concentration of gold nanoparticles from UV–Vis spectra. Anal Chem 79:4215–4221

44. Kim J-H, Lavin BW, Burnett RD, Boote BW (2011) Controlled synthesis of gold nanoparticles by fluorescent light irradiation. Nanotechnology 22:p285602–p285607

45. Moskovits M, Srnová-Sloufová I, Vlcková B (2002) Bimetallic Ag–Au nanoparticles: extracting meaningful optical constants from the surface-plasmon extinction spectrum. J Chem Phys 116:10435–10446

46. Liz-Marzan LM (2006) Tailoring surface plasmons through the morphology and assembly of metal nanoparticles. Langmuir 22:32–41

47. Hutter E, Fendler JH (2002) Size quantized formation and self-assembly of gold encased silver nanoparticles. Chem Commun:378–379

48. Ramos M, Ferrer DA, Chianelli RR, Correa V, Serrano-Matos J, Flores S (2011) Synthesis of Ag-Au nanoparticles by galvanic replacement and their morphological studies by HRTEM and computational modeling. J Nanomater 2011:5 pages

49. Mie G (1908) Contributions to the optics of turbid media, particularly of colloidal metal solutions. Ann Phys 25:377–445

50. Rodriguez-Fernandez J, Perez-Juste J, Garcia de Abajo FJ, Liz-Marzan LM (2006) Seeded growth of submicron Au colloids with quadrupole plasmon resonance modes. Langmuir 22:7007–7010

51. Sanchez-Gaytan B, Park S-J (2010) Spiky gold nanoshells. Langmuir 26:19170–19174